

Stability of magnetosonic waves in an anti-loss cone plasma

C Venugopal^{1*}, S George¹, V R Rajeev¹, R Jayapal¹, M J Kurian² and C P Anilkumar³

¹School of Pure and Applied Physics, Mahatma Gandhi University, Priyadarshini Hills, Kottayam 686 560, Kerala, India

²Department of Physics, Catholicate College, Mahatma Gandhi University, Pathnamthitta 689 645, Kerala, India

³Equatorial Geophysical Laboratory, Indian Institute of Geomagnetism, Krishnapuram, Tirunelveli 627 011, Tamil Nadu, India

Received: 06 February 2013 / Accepted: 03 May 2013 / Published online: 17 May 2013

Abstract: We have studied the stability of magnetosonic wave in a plasma, where the ions and electrons are described by anti-loss cone (ALC) distributions. Our studies indicate that the magnetosonic waves produced by ions and electrons with ALC distributions are in the higher frequency end within the range of frequencies, as observed by the Combined Release and Radiation Effects Satellite spacecraft. They are weakly damped and can, therefore, travel long distances. These waves are expected to play an important role in the acceleration of radiation belt electrons.

Keywords: Magnetosonic wave; Dispersion relation; Stability; Anti-loss cone plasma; Radiation belt electrons

PACS Nos.: 52.27.Aj; 52.35.-g; 52.35.Qz

1. Introduction

Field fluctuations, with frequencies close to the proton gyrofrequency and its harmonics and up to the lower hybrid frequency, have been observed at radial distances of 2–8 R_E around the geomagnetic equator in the magnetosphere [1, 2]. These waves, observed mainly in the afternoon and pre-midnight sectors, propagate nearly perpendicular to the magnetic field. Observational [3, 4] and theoretical [5–7] studies indicate that the wave is driven by energetic (of the order of tens of keV) protons with ring like distributions. More recent observations are made by the CLUSTER satellite in the plasma sheet boundary layer (PSBL) [8].

These waves, initially called “equatorial noise” [1] are now referred to as “magnetosonic waves”. In contrast to their generation mechanism in the PSBL, magnetosonic waves in the inner magnetosphere are driven by a tenuous, energetic (of tens of keV) protons, in the presence of a cold background plasma (electrons and ions with energies of ~ 1 eV) [3, 9]. Other studies on these waves, as observed by the Combined Release and Radiation Effects Satellite (CRRES) spacecraft from the proton gyrofrequency up to the upper hybrid wave frequency, have been restricted to a

frequency range between $0.5 f_{LHR}$ and f_{LHR} (f_{LHR} is the lower hybrid frequency). Emissions are observed to occur most of the time outside plasmopause; the most intense being in region of $L = 3–4$ [4]. These waves are generally believed to contribute to the transverse heating of protons [10, 11] and the acceleration of radiation belt electrons [12–14]. Other proposed mechanism is a new variant of the theory of magnetospheric resonator for magnetosonic waves [15] and the numerical investigations of temporal evolution of cylindrical magnetoacoustic waves in planetary magnetospheres [16]. It has also been shown that the slow magnetosonic perturbations generated in vicinity of magnetopause can be transformed into fast magnetosonic wave, which can then propagate into the magnetosheath [17]. The association of Pc5 pulsations with the Alfvén and magnetosonic waves has also been studied [18]. The dispersion characteristics of low frequency waves in multi-ion plasmas have also been investigated recently [19]. Other relevant studies are the investigations of effect of an electric field on electromagnetic ion cyclotron (EMIC) wave [20] where it is found that the electric field control the growth rate of these waves, while the steep loss cone distribution enhance the growth rate and perpendicular heating of the ions. Wave propagation around the electron cyclotron frequency has also been investigated [21].

In magnetopause, the loss cone cannot be completely empty since a fraction of the loss cone particles is scattered

*Corresponding author, E-mail: cvgmphys@yahoo.co.in

back into the loss cone. Besides, newer particles may be continuously entering the loss cone through convection or pitch angle diffusion. Thus realization of a loss cone distribution is not easy in practice. Wu [22], therefore, has suggested a partially filled loss cone distribution that could be constructed by subtracting two Maxwellians. This new distribution is called the anti-loss cone (ALC) distribution, the existence of which has been predicted by Roederer [23] and is characterized by a deficit of particles with $v_{\parallel} \approx 0$. This distribution has been observed to be present beyond the plasmasphere and near earth plasmashet [24], the extra-terrestrial ring current region [25] and the central plasma sheet (CPS) [26]. In addition, protons streaming along magnetic field lines, with maxima near 0° or 180° pitch angle are well described by ALC distributions [27]. Such streaming protons have been observed in the dayside magnetosphere [28] and the polar cusp [29]. Another instance is that by the SCATHA satellite, which observed electrons with a pronounced pitch angle minimum of 90° [30]. Again, in a modeling study, Ashour-Abdalla et al. [31] have reproduced the essential features of both large scale distributions of ions in the geomagnetic tail and their small scale structures in configuration and velocity space. A very important conclusion of their study is that the plasma in the CPS exhibits a ALC distribution. More recently, INTERBALL observations of the low latitude boundary layer (LLBL) has revealed that the ions are field aligned and counter streaming [32]. It is thus evident that the plasma in the inner regions of the magnetosphere can be well modeled by ALC distribution.

Instabilities driven by ALC distributions have been studied by a number of researchers: Kennel et al. [33] and Nambu and Watanabe [34] have studied the ion acoustic and the electrostatic ion cyclotron waves in such plasmas to explain the high frequency waves observed in the magnetosphere. That this distribution is unstable to electrostatic and electromagnetic drift instabilities has been demonstrated [25, 35–37]. The whistler mode has also been shown to be unstable in this plasma [38, 39]. Other wave modes investigated using this distribution function are the lower hybrid and modified electron acoustic instabilities [40] and the electromagnetic ion cyclotron wave [41].

We have studied the stability of magnetosonic wave in a plasma, where the ions and electrons are described by anti-loss cone distributions: the motivation is conjecture of Meredith et al. [4] that magnetosonic waves produced in remote regions propagate both radially and azimuthally. Our studies indicate that the magnetosonic waves produced by ions and electrons with ALC distributions are in the higher frequency end within the range of frequencies observed by the CRRES spacecraft. They are weakly damped and can, therefore, travel long distances as conjectured in [4].

2. The general dispersion formula

We are interested in the propagation and stability of the magnetosonic wave in a plasma where both the ions and electrons are described by ALC distributions.

For this purpose we consider a homogeneous, uniformly magnetized plasma of ions and electrons in an external magnetic field $B = B_0 \hat{z}$. In presence of a wave described by (ω, \vec{k}) the response of the plasma medium is described by the Vlasov equation

$$\frac{\partial f_\alpha}{\partial t} + \vec{v} \cdot \nabla f_\alpha + \frac{q_\alpha}{m_\alpha} \left[\vec{E} + \frac{\vec{v}_\alpha \times \vec{B}^T}{c} \right] \cdot \frac{\partial f_\alpha}{\partial \vec{v}} = 0 \quad (1)$$

where $\alpha = i$ (ions) or e (electrons). $\vec{E}(r, t)$ and $\vec{B}(r, t)$ are the self consistent electric and magnetic fields with $\vec{B}^T = \vec{B}_0 + \vec{B}(r, t)$. q_α and m_α denote, respectively, the charge and mass of species α .

We transform Eq. (1) to cylindrical coordinates in velocity space, namely $(v_\perp, 0, v_\parallel)$. Neglecting the magnetic component of the wave in comparison to electrical component (as it is smaller by a factor of v/c) and assuming a perturbation of the form $\exp[i(\vec{k} \cdot \vec{r} - \omega t)]$, the Fourier–Laplace transform of the linearised form of Eq. (1) [42], is

$$i(\vec{k} \cdot \vec{v} - \omega) f_{\alpha k \omega} - \omega_{c\alpha} \frac{\partial f_{\alpha k \omega}}{\partial \phi} = -\frac{q_\alpha}{m_\alpha} \vec{E}_{k \omega} \cdot \frac{\partial f_{\alpha 0}}{\partial \vec{v}} \quad (2)$$

In Eq. (2) $\omega_{c\alpha} = |q_\alpha| B_0 / (m_\alpha c)$ is the gyrofrequency, B_0 is the ambient magnetic field and c is the velocity of light. We assume \vec{k} to lie within the x–z plane and $\vec{k} = (k_\perp, 0, k_\parallel)$. Using the same notation as in [42] and defining

$$\rho_\perp(\parallel) = \frac{k_\perp v_\perp(\parallel)}{\omega_{c\alpha}}, \quad s = \frac{\omega}{\omega_{c\alpha}}, \quad f \equiv f_{\alpha k \omega} \quad (3)$$

and

$$\Lambda(\phi) = \frac{q_\alpha}{m_\alpha \omega_{c\alpha}} E_{k \omega} \cdot \frac{\partial f_{\alpha 0}(v_\perp^2, v_\parallel^2)}{\partial \vec{v}}, \quad (4)$$

we can write Eq. (2) as

$$\frac{\partial f}{\partial \phi} = i(\rho_\perp \cos(\phi) + \rho_\parallel - s)f + \Lambda(\phi) \quad (5)$$

The solution to Eq. (5) is given by [42]

$$f = \exp[i(\rho_\perp \sin(\phi) + \rho_\parallel \phi - s\phi)] \cdot \int d\phi \Lambda(\phi) \exp[-i(\rho_\perp \sin(\phi) + \rho_\parallel \phi - s\phi)] \quad (6)$$

We now need an explicit form for the particle distribution function $f_{\alpha 0}$. In this paper we choose

$$f_{x0} = f_{x00} \exp(-v_{\perp}^2 \alpha_{\perp\alpha}) [\exp(-v_{\parallel}^2 \alpha_{t\alpha}) - \rho_{\alpha} \exp(-v_{\parallel}^2 \alpha_{m\alpha})] \quad (7)$$

In Eq. (7) $f_{x00} = \pi^{-3/2} \alpha_{\perp\alpha} (\alpha_{t\alpha}^{-1/2} - \rho_{\alpha} \alpha_{m\alpha}^{-1/2})^{-1}$ is the normalization constant, while, $\alpha_{\perp\alpha} = (m_{\alpha}/2k_B T_{\perp\alpha})$ and $\alpha_{m\alpha} = (m_{\alpha}/2k_B T_{m\alpha})$. T_t and T_m denote the temperatures of the trapped and missing particles, T_{\perp} is the temperature perpendicular to the magnetic field, k_B is the Boltzmann's constant and the parameter ρ controls the strength of the anti-loss cone. We thus get

$$\Lambda(\phi) = \Lambda_1 \cos(\phi) + \Lambda_2 \sin(\phi) + \Lambda_3 \quad (8)$$

with

$$\Lambda_1 = -\frac{q_{\alpha}}{m_{\alpha} \omega_{c\alpha}} \vec{E}_{xk\omega} (2v_{\perp} \alpha_{\perp}) f_{x0}$$

$$\Lambda_2 = -\frac{q_{\alpha}}{m_{\alpha} \omega_{c\alpha}} E_{yk\omega} (2v_{\perp} \alpha_{\perp}) f_{x0}$$

and

$$\Lambda_3 = -\frac{q_{\alpha}}{m_{\alpha} \omega_{c\alpha}} E_{zk\omega} f_{x00} (2v_{\parallel} \alpha_t) \exp(-v_{\perp}^2 \alpha_{\perp\alpha}) \cdot \left[\exp(-v_{\parallel}^2 \alpha_{t\alpha}) - \rho_{\alpha} \frac{\alpha_{m\alpha}}{\alpha_{t\alpha}} \exp(-v_{\parallel}^2 \alpha_{m\alpha}) \right] \quad (9)$$

Using a well known identity connecting the exponential and Bessel's function J_n , we can write down the solution of Eq. (6) as:

$$f_{xk\omega} = -i \frac{q_{\alpha} \alpha_{\perp\alpha}}{m_{\alpha}} \sum_{n,l} \frac{J_n(\rho_{\perp\alpha}) \exp[i(n-l)\phi]}{k_{\parallel} v_{\parallel} - \omega + l\omega_{c\alpha}} A_{zk\omega} \quad (10)$$

where

$$A_{zk\omega} = a_x E_{xk\omega} + a_y E_{yk\omega} + a_z E_{zk\omega} \quad (11)$$

with

$$a_x = v_{\perp} [J_{l+1}(\rho_{\perp\alpha}) + J_{l-1}(\rho_{\perp\alpha})] f_{x0}$$

$$a_y = -iv_{\perp} [J_{l+1}(\rho_{\perp\alpha}) - J_{l-1}(\rho_{\perp\alpha})] f_{x0}$$

and

$$a_z = J_l(\rho_{\perp\alpha}) 2v_{\parallel} \frac{\alpha_{t\alpha}}{\alpha_{\perp\alpha}} f_{x00} \exp(-v_{\perp}^2 \alpha_{\perp\alpha}) \cdot \left[\exp(-v_{\parallel}^2 \alpha_{t\alpha}) - \rho_{\alpha} \frac{\alpha_{m\alpha}}{\alpha_{t\alpha}} \exp(-v_{\parallel}^2 \alpha_{m\alpha}) \right] \quad (12)$$

As a check on our results, we note that Eq. (12) reduces to the corresponding equation in [42] if $\alpha_{\perp\alpha} = \alpha_{t\alpha}$ and $\rho_{\alpha} = 0$. $f_{zk\omega}$ of Eq. (10) that can be used to calculate the perturbed current is defined by

$$J_{k\omega} = \sum_{\alpha} n_{\alpha 0} q_{\alpha} \int \vec{v} f_{zk\omega} d\vec{v} \equiv \vec{\sigma} \cdot \vec{E} \quad (13)$$

where general expression for the components of the conductivity tensor are [42]

$$\sigma_{\mu\nu} = -i \sum_{\alpha} \frac{n_{\alpha} q_{\alpha}^2 \alpha_{\perp\alpha}}{m_{\alpha}} \sum_{n,l} \int \frac{v_{\mu} a_{\nu} J_n(\rho_{\perp\alpha}) \exp[i(n-l)\phi]}{k_{\parallel} v_{\parallel} - \omega + l\omega_{c\alpha}} f_{x0} d\vec{v} \quad (14)$$

3. Dispersion formula for magnetosonic waves

We consider the near perpendicular propagation of an electromagnetic wave in a plasma, where both the ions and electrons are described by ALC distribution. We assume that $\omega \ll \omega_{ci}$, $E_x = E_z = 0$, ($E_y \neq 0$), $\vec{k} = \hat{x}k_{\perp} + \hat{z}k_{\parallel}$ with $k_{\perp}^2 \gg k_{\parallel}^2$. The dispersion formula for the magnetosonic wave is given by [42]

$$\frac{c^2 k^2}{\omega^2} = 1 + \chi_{yy} \quad (15)$$

where

$$\chi_{yy} = \frac{4\pi i}{\omega} \sigma_{yy} \quad (16)$$

Using Eq. (14) and carrying out the $d\phi$ -integration, we get the final expression for σ_{yy} as

$$\sigma_{yy} = -i \sum_{\alpha} \omega_{p\alpha}^2 \alpha_{\perp\alpha} \sum_1 \int \frac{[J'_l(\rho_{\perp\alpha})]^2}{k_{\parallel} v_{\parallel} - \omega + l\omega_{c\alpha}} f_{x0} v_{\perp}^3 dv_{\perp} dv_{\parallel} \quad (17)$$

where J'_l is the derivative of the Bessel function. Substituting for f_{x0} from Eq. (7) and carrying out the dv_{\perp} -integration using the basic integral [43]

$$I(\alpha, \beta) = \int_0^{\infty} dv_{\perp} v_{\perp} \exp(-v_{\perp}^2 \alpha_{\perp}) J_l(av_{\perp}) J_l(bv_{\perp}) = \frac{1}{2\alpha_{\perp}} \exp\left[-\frac{(a^2 + b^2)}{4\alpha_{\perp}}\right] I_l\left(\frac{ab}{2\alpha_{\perp}}\right) \quad (18)$$

and the dv_{\parallel} -integration using the plasma dispersion function, we arrive at the final form for χ_{yy} as

$$\chi_{yy} = \frac{1}{\omega} \sum_{\alpha} \frac{\omega_{p\alpha}^2}{k_{\parallel} \alpha_{t\alpha}^{-1/2}} \frac{1}{1 - \rho_{\alpha} \left(\frac{T_{m\alpha}}{T_{t\alpha}}\right)^{1/2}} \Lambda(L_{\perp\alpha}) [Z(\zeta_{t\alpha}) - \rho_{\alpha} Z(\zeta_{m\alpha})] \quad (19)$$

In Eq. (19)

$$\Lambda(L_{\perp\alpha}) = \exp(-L_{\perp\alpha}) [L_{\perp\alpha} I_1(L_{\perp\alpha}) + (1 - 2L_{\perp\alpha}) \frac{d}{dL_{\perp\alpha}} I_1(L_{\perp\alpha}) + L_{\perp\alpha} \frac{d^2}{dL_{\perp\alpha}^2} I_1(L_{\perp\alpha})] \quad (20)$$

with

$$L_{\perp\alpha} = \frac{k_{\perp}^2}{2\omega_{c\alpha}^2 \alpha_{\perp\alpha}} \quad (21)$$

I_l is the modified Bessel function. The arguments of the plasma dispersion function are

$$\zeta_{t(m)} = \frac{(\omega - l\omega_{c\alpha})\alpha_{t(m)}^{1/2}}{k_{\parallel}} \quad (22)$$

3.1. The dispersion relation and growth/damping rate

In this section, we have derived the dispersion relation and the expression for the growth/damping rate for the magnetosonic wave.

For near perpendicular propagation, $k_{\parallel} \ll 1$; hence from Eq. (22), $\zeta_{t(m)} \gg 1$. The asymptotic expansion of the plasma dispersion function is thus needed and it is given by [44]

$$Z(\zeta) \approx -\frac{1}{\zeta} - \frac{1}{2} \frac{1}{\zeta^3} \dots + i\sqrt{\pi} \frac{k}{|k|} \exp(-\zeta^2) \quad (23)$$

We also assume $L_{\perp i} \ll 1$ so that both the exponential and the modified Bessel functions in Eq. (20) can be expanded as a power series. Substituting Eq. (23) and the power series expansion of Eq. (20) and considering only $l = 0$ and ± 1 contributions from both electrons and ions, Eq. (19) in conjunction with Eq. (15) yields the following dispersion relation for propagation of magnetosonic waves:

$$\begin{aligned} \frac{k^2 c^2}{\omega^2} - 1 + \frac{\omega_{pe}^2}{\omega^2} \left[2L_{\perp e} + \frac{\omega^2}{\omega^2 - \omega_{ce}^2} (1 - 3L_{\perp e}) \right] \\ + \frac{\omega_{pi}^2}{\omega^2} \left[2L_{\perp i} + \frac{\omega^2}{\omega^2 - \omega_{ci}^2} (1 - 3L_{\perp i}) \right] \\ = 0 \end{aligned} \quad (24)$$

As a check on Eq. (24) we note that for $L_{\perp e} = L_{\perp i} = 0$ (cold plasma) and for $\omega^2 \ll \omega_{ci}^2$ it reduces to

$$\omega^2 = \frac{k^2 v_A^2}{1 + \frac{v_A^2}{c^2}} \quad (25)$$

which is the dispersion relation for the fast magnetosonic wave [45]. In Eq. (25), v_A is the Alfvén velocity defined by $v_A^2 = B_0^2 / (4\pi n_0 m_i)$. On the other hand, for $L_{\perp i} = 0$ but $L_{\perp e} \neq 0$ (cold ions and hot electrons), Eq. (24) can be shown to reduce to

$$\frac{\omega^2}{c^2 k^2} = \frac{v_A^2 + v_S^2}{v_A^2 + c^2} \quad (26)$$

which is the same as given by Chen [46] for magnetoacoustic waves. In Eq. (26), v_S is the ion acoustic speed defined by $v_S = (2T_e/m_i)^{1/2}$. Using the imaginary part of dispersion function expansion given by Eq. (23) and

writing $\omega = \omega_r + i\omega_i$, Eqs. (15) and (19) yield the expression for the growth/damping rate as

$$\begin{aligned} \omega_i = \\ - \frac{\sqrt{\pi}}{k_{\parallel}} \sum_{\alpha=e,i} \left\{ \frac{\omega_{p\alpha}^2 L_{\perp\alpha} \alpha_{t\alpha}^{1/2}}{\left[1 - \rho_{\alpha} \left(\frac{T_m}{T_i} \right)_{\alpha} \right]^{1/2}} \left[\exp(-\zeta_{t\alpha 0}^2) - \rho_{\alpha} \exp(-\zeta_{m\alpha 0}^2) \right] \right\} \end{aligned} \quad (27)$$

In Eq. (27), we have retained only the $l = 0$ electron and ion contributions. As a check on Eq. (27), we note that for $\rho_i = \rho_e = 0$ it reduces to the corresponding expression in [42]. It is also seen from Eq. (27) that the magnetosonic wave is always damped, the damping being dominated by electrons. However, as is obvious from Eq. (27), the damping is lesser in a plasma described by an ALC distribution than in a plasma described by a Maxwellian distribution.

4. Results

The dispersion relation given by Eq. (24) and the expression for the damping rate [Eq. (27)] have been derived with restrictive assumptions. To relax these conditions, it is decided to solve the dispersion relation numerically. Hence the dispersion relation given in Eq. (15) is set up using Eq. (19) and solved using the IMSL routine ZANALY which calculates the complex zeros of a function $f(z)$ using Muller's method [47]. It may also be noted at this point that a subtracted Maxwellian distribution is used in a simulation study of magnetosonic waves [48].

Magnetosonic waves starting from the proton gyrofrequency up to the upper hybrid frequency have been observed by the CRRES spacecraft. However, the survey of Meredith et al. [4] concentrates on waves between $0.5 f_{LHR}$ and f_{LHR} to provide a balance between including the strongest emissions, in the region of $L = 3-4$ and provides a reasonable coverage in L . It may also be mentioned here that magnetosonic waves have also been observed even in the absence of proton rings [49]. Also observational evidence generally suggests that these waves are associated with energetic protons of energies of 10 s of keV [3, 4]. Thus the parameters used in our computations are as follows: the background magnetic field $B_0 = 0.31/L^3$ with $L = 4$, ion and electron temperatures respectively equivalent to 25 keV and 100 eV and an ion density of 10 cm^{-3} . The damping rate is studied as a function of the parameters of the ALC distribution namely ρ , T_m , T_i , etc.

Figure 1 is a plot of the damping rate versus $k_{\perp} r_L$ (r_L being the ion Larmor radius) as a function of the propagation angle ϑ for $(T_m/T_i)_i = (T_m/T_i)_e = 0.9$, $\rho_e = \rho_i = 0.5$ and $(T_{\perp}/T_i)_i = 10.0$. The continuous curve is for a propagation angle of 65° and the dashed one for an angle of

85°. As can be seen from the figure, the damping rate is generally larger for near perpendicular propagation angles, with the maximum shifting towards larger $k_{\perp}r_L$ as the propagation angle increases.

Figure 2 is a plot of the damping rate versus $k_{\perp}r_L$ as a function of the ALC index ρ ; the other parameters for the figure being $\vartheta = 85^\circ$, $(T_m/T_t)_i = (T_m/T_t)_e = 0.9$ and $(T_{\perp}/T_t)_i = 10.0$. The dashed curve is for $\rho_e = \rho_i = 0$ (Maxwellian plasma) and the continuous curve for $\rho_e = \rho_i = 0.9$. We see that the damping rate is a maximum for a Maxwellian plasma; this result being in agreement with the conclusion from Eq. (27).

Figure 3 is a plot of the damping rate versus $k_{\perp}r_L$ as a function of (T_m/T_t) with a propagation angle $\vartheta = 85^\circ$. The other parameters are: $(T_{\perp}/T_t)_i = 10.0$, $\rho_e = \rho_i = 0.9$; the dashed curve is for $(T_m/T_t)_i = (T_m/T_t)_e = 0.1$ while the continuous curve is for $(T_m/T_t)_i = (T_m/T_t)_e = 0.9$. We find that peak value of the damping rate is smaller for larger values of (T_m/T_t) ; there is also a shift in the peak value to larger $k_{\perp}r_L$ as (T_m/T_t) decreases.

5. Discussion

Fast magnetosonic waves in the magnetosphere are expected to play an important role in the scattering and acceleration of radiation belt electrons [13]. They are believed responsible for accelerating electrons from ~ 10 keV to a few MeV on a time scale of 1–2 days and hence play an important role in radiation belt dynamics [4, 14].

The study of Meredith et al. [4] which is restricted to magnetosonic waves of frequencies between $0.5 f_{LHR}$ and f_{LHR} , for reasons already mentioned, revealed low energy (ring energy $E_R < 30$ keV but with $E_R > E_A$, the Alfvén energy) proton rings to be closely associated with the observation of magnetosonic waves both inside plasma-pause as well as outside the plasma-pause on the dusk side. Ion ring distributions are therefore put forward as a likely source of generation for these waves. However, the observation of proton rings with energies $E_R < E_A$ suggests that rings are not the only source for these waves. One of the explanations offered by Meredith et al. [4] is the propagation of these waves over long distances, both radially and azimuthally, from a remote source region.

In a recent analytic study, based on Snell's law, it is found that untrapped waves launched inside and outside the plasmasphere could travel azimuthally 0–4 and 0–7 h in local times respectively. This substantial radial and azimuthal propagation may account for the presence of magnetosonic waves far away from the source region [49].

Our numeric results show a frequency range extending from $0.38 f_{LHR}$ to $1.94 f_{LHR}$, in broad agreement with observations at the higher frequency end in Meredith et al. [4]. Since they are weakly damped, they can propagate both radially and azimuthally as required [4, 49]. The local acceleration of electrons is expected to occur over a time scale of 1–2 days [4, 14]; the waves should therefore be weakly damped for an effective absorption of wave energy. Since our results show that the wave is weakly damped, such an effective transfer of energy is plausible.

Fig. 1 Plot of damping rate versus normalised wavelength $k_{\perp}r_L$ for $(T_m/T_t)_i = (T_m/T_t)_e = 0.9$, $\rho_i = \rho_e = 0.5$, $(T_{\perp}/T_t)_i = 10.0$. The continuous curve is for a propagation angle $\vartheta = 65^\circ$; the dashed curve is for $\vartheta = 85^\circ$. The numerical values have been multiplied by $1.0e+05$

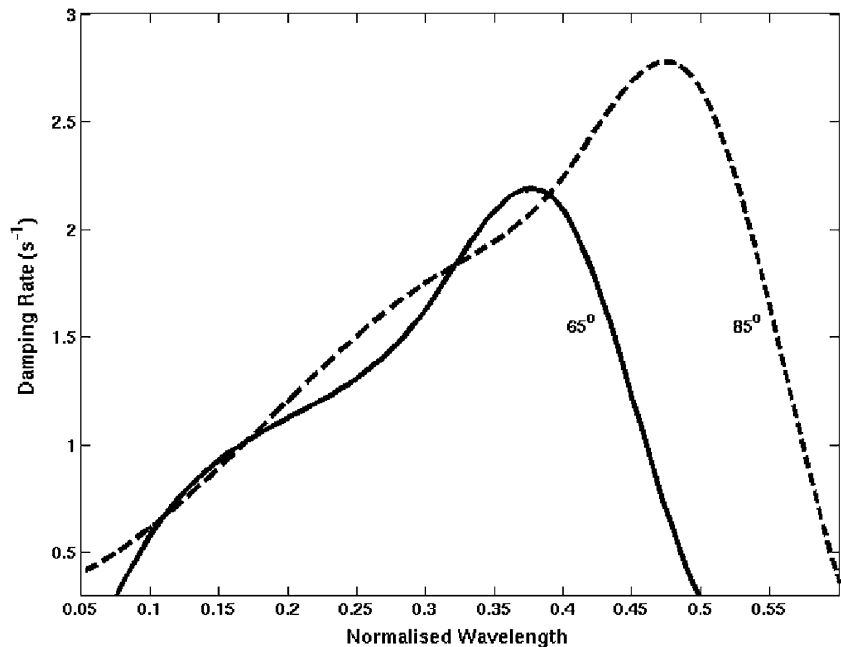


Fig. 2 Plot of damping rate versus normalised wavelength $k_{\perp}r_L$ for $(T_m/T_i)_i = (T_m/T_i)_e = 0.9$, $(T_{\perp}/T_i)_i = 10.0$ and a propagation angle $\vartheta = 85^\circ$. The *continuous curve* is for an ALC plasma with $\rho_i = \rho_e = 0.9$ and the *dashed curve* is for a Maxwellian plasma $\rho_i = \rho_e = 0$. The numerical values have been multiplied by $1.0e+05$

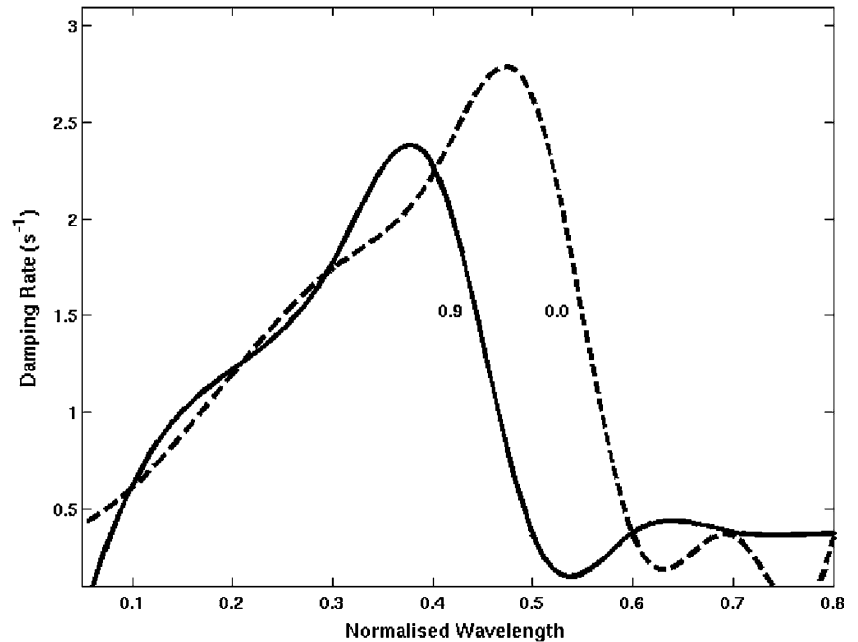
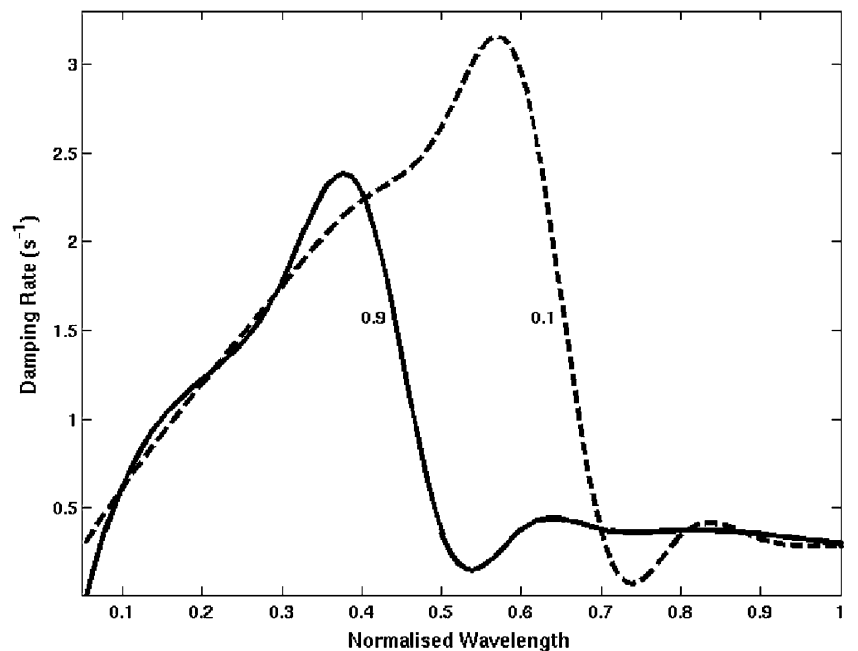


Fig. 3 Plot of damping rate versus normalised wavelength $k_{\perp}r_L$ for $\rho_i = \rho_e = 0.9$, $(T_{\perp}/T_i)_i = 10.0$ and a propagation angle $\vartheta = 85^\circ$. The *dashed curve* is for $(T_m/T_i)_i = (T_m/T_i)_e = 0.1$ and the *continuous curve* for $(T_m/T_i)_i = (T_m/T_i)_e = 0.9$. The numerical values have been multiplied by $1.0e+05$



6. Conclusions

We have studied the stability of magnetosonic wave in a plasma where the ions and electrons are described by anti-loss cone distributions. We have derived expressions for both the dispersion relation and the growth/damping rate in a plasma where both the ions and electrons are described by anti-loss cone distribution functions. Real part of the dispersion relation is shown to reduce to standard results under limiting conditions. Our numeric calculations show that the

waves have, indeed the correct frequency range at the higher end of the wave spectrum. They are weakly damped and can, therefore, travel long distances as conjectured in [4]. Due to their weak damping they can effectively interact with electrons; they can thus be considered as one of the agents for the acceleration of electrons.

Acknowledgments Authors at SPAP acknowledge financial assistance by the UGC under its Special Assistance Programme and the DST under its FIST and PURSE Programmes.

References

- [1] C T Russell, R E Holzer and E J Smith *J. Geophys. Res.* **75** 755 (1970)
- [2] O Santolik, J S Pickett, D A Gurnett, M Maksimovic and N Cornilleau-Wehrin *J. Geophys. Res.* **107** 1495 (2002)
- [3] S Perraut, et al., *J. Geophys. Res.* **87** 6219 (1982)
- [4] N P Meredith, R B Horne and R R Anderson *J. Geophys. Res.* **113** 6213 (2008)
- [5] A V Gul'elmi, B I Klaine and A S Potapov *Planet. Space Sci.* **23** 279 (1975)
- [6] K G McClements, R O Dendy and C N Lashmore-Davies *J. Geophys. Res.* **99** 23685 (1994)
- [7] L Chen, R M Thorne, V K Jordanova and R B Horne *J. Geophys. Res.* **115** 11222 (2010)
- [8] R E Denton et al., *J. Geophys. Res.* **115** 12224 (2010)
- [9] S Boardsen, D Gallagher, D A Gurnett, W K Peterson and J L Green *J. Geophys. Res.* **97** 14967 (1992)
- [10] S A Curtis *J. Geophys. Res.* **90** 1765 (1985)
- [11] R B Horne, G V Wheeler and H St C K Alleyne *J. Geophys. Res.* **105** 27597 (2000)
- [12] R B Horne and R M Thorne *Geophys. Res. Lett.* **25** 3011 (1998)
- [13] Y Y Shprits *Geophys. Res. Lett.* **36** L12106 (2009)
- [14] J Bortnik and R M Thorne *J. Geophys. Res.* **115** 07213 (2010)
- [15] A S Leonovich and V A Mazur *Cosmic Research* **46** 327 (2008)
- [16] W Masood, H Rizvi, N Jehan and M Siddiq *Astrophys. Space Sci.* **335** 405 (2011)
- [17] N Borisov and M Franz *Nonlin. Processes Geophys.* **18** 209 (2011)
- [18] V B Belakhovsky, V A Pilipenko and A E Kozlovsky *Physics of Auroral Phenomena*, Proc. XXXIII Annual Seminar **69** (Apatity: Russian Academy of Science) (2011)
- [19] C Venugopal, M J Kurian, E S Devi, P J Jessy, C P Anilkumar and G Renuka *Indian J. Phys.* **84** 319 (2010)
- [20] S Patel, P Varma and M S Tiwari *Indian J. Phys.* **86** 535 (2012)
- [21] N Nimje, S Dubey and S Ghosh *Indian J. Phys.* **86** 749 (2012)
- [22] C S Wu *Space Sci. Rev.* **41** 215 (1985)
- [23] J G Roederer *J. Geophys. Res.* **72** 981 (1967)
- [24] H I West Jr, R M Buck and J R Walton *J. Geophys. Res.* **78** 1064 (1973)
- [25] B Buti *J. Plasma Phys.* **15** 105 (1976)
- [26] M Ashour-Abdalla, J Buchner and L M Zelenyi *J. Geophys. Res.* **96** 1601 (1991)
- [27] K G Bhatia and G S Lakhina *Astrophys. Space Sci.* **68** 175 (1980)
- [28] H Borg, et al. *Space Sci. Rev.* **22** 511 (1978)
- [29] D A Gurnett and L A Frank *J. Geophys. Res.* **83** 1447 (1978)
- [30] H C Koons and J F Fennel *J. Geophys. Res.* **88** 6221 (1983)
- [31] M Ashour-Abdalla, J Berchem and J Buchner *Geophys. Res. Lett.* **18** 1603 (1991)
- [32] J-A Sauvaud, et al. *Ann. Geophys.* **15** 587 (1997)
- [33] C F Kennel, R W Fredricks and F L Scarf *Particles and Fields in the Magnetosphere* (ed.) B M McCormac (Dordrecht: D Riedel Pub. Co.) (1970)
- [34] M Nambu and T Watanabe *Geophys. Res. Lett.* **2** 176 (1975)
- [35] B Buti *J. Geophys. Res.* **81** 5363 (1976b)
- [36] B Buti *J. Plasma Phys.* **16** 73 (1976c)
- [37] B Buti *J. Geophys. Res.* **81** 6221 (1976d)
- [38] G S Lakhina *Planet. Space Sci.* **25** 598 (1977)
- [39] P R Prince and G Renuka *Indian J. Radio Space Phys.* **36** 318 (2007)
- [40] K G Bhatia and G S Lakhina *J. Plasma Phys.* **19** 193 (1978)
- [41] C Venugopal, S Antony, N P Shibu George, G Renuka and G J Bailey *Adv. Space Res.* **17** 10245 (1996)
- [42] M Salimullah, M I U Khan, M K Islam, M R Amin and P K Shukla *Phys. Scr.* **73** 320 (2006)
- [43] I S Gradshteyn and I M Ryzhik *Table of Integrals, Series and Products* 6th edn. (eds.) A Jeffrey and D Zwillinger (New York: Academic Press) (2000)
- [44] B D Fried and S D Conte *The Plasma Dispersion Function* (New York: Academic Press) (1961)
- [45] D R Nicholson *Introduction to Plasma Theory* (New York: John Wiley & Sons) (1983)
- [46] F F Chen *Introduction to Plasma Physics and Controlled Fusion* (New York: Plenum Press) (1974)
- [47] *Visual Numerics* www.roguewave.com (2012)
- [48] K Liu, S P Gary and D Winske *J. Geophys. Res.* **116** 07212 (2011)
- [49] L Chen and R M Thorne *Geophys. Res. Lett.* **39** L14102 (2012)